Asian Journal of Chemistry; Vol. 25, No. 8 (2013), 4137-4140

ASIAN JOURNAL OF CHEMISTRY

http://dx.doi.org/10.14233/ajchem.2013.11031

Effect of pH at Early Formed Structures in Cobalt Electrodeposition

SAHARI ALI* and MOKHTARI SALIM

Laboratoire de Chimie, Ingénierie Moléculaire et Nanostructures, Université de Sétif, Setif, Algeria

*Corresponding author: Fax: +213 36 925133; Tel: +213 36 723787; E-mail: sahariali2000@yahoo.com

(*Received*: 15 January 2012; *Accepted*: 4 February 2013) AJC-12912

The electrodeposition of cobalt on platinum wafer substrates was studied *versus* electrolyte pH. The crystallographic structure of electrodeposited cobalt films found to be very sensitive on the electrolyte pH value. During the first stage of growth, at pH = 2 a mixture of Co_{fcc} and Co_{hcp} are formed with the prevailing Co_{fcc} phase. By increasing the pH ($3.0 < pH < 4.0$), Co_{hcp} becomes the major fraction with good crystallization state and large grain sizes. Electrochemical impedance spectroscopy technique was used to describe the interface's behaviour and the passage steps of electrodeposition process. It was found that at pH = 2, the impedance spectra are characterized by the presence of a semicircle feature at high frequencies and by complex inductance at low frequencies. At pH ($3.0 < pH < 4.0$), the inductive feature disappears and replaced by capacitive feature indicating the control of electrodeposition by the deposition process.

Key Words: Electrochemical impedance spectroscopy, Instantaneous nucleation, Cobalt, Electrodeposition.

INTRODUCTION

The electrodeposition of transition metals such as Co, in a metallic matrix of Cu, Pt, Au or Ag both in the form of coupled metallic multilayers and in the form of heterogeneous alloys, has attracted considerable attention for its potential applicability to many modern technologies[1-5]. The investigation of the structural properties of the electrodeposits of cobalt has shown[6] that they are developed mainly in different selective phases, depending on the electrodeposition conditions[7] *e.g.*, nature of electrolyte, pH, bath temperature, current density, stirring and addition of organic compounds. Also, the physico-chemical properties electrodeposits are greatly affected by the above electrodeposition conditions[8]. One of important parameters of these conditions is the pH of electrolyte which plays a great role in the process of electrodeposition. To give idea for example how generally pH affects the cathodes area is in acidic electrolytes the presence of hydrogen, H^+ is reduced to H_{ads}, which strongly adheres to the electrode surface and inhibits further reduction. After charge transfer the adsorbed hydrogen is liberate as H_2 and the pH of the nearest cathode area is considerably modified by consummation of hydrogen ions. To limit this phenomenon, within the electrolyte medium boric acid is added in appropriation quantities[9-11]. The influence of the pH is quite obvious, at macroscopic (electroplating) process, the increasing of pH is one consequence of formation of undesirably species as metal's hydroxide at many cases these species confer the low grade to electrodeposits[12] (poor conductivity, rough surface, *etc.*). In other way and at microscopic scale (nanoparticles formation), it is reported that many properties (magnetic as good example) of thin films depend both on the orientation and grain size of the crystals[13,14]. In this work we show that structure and grain sizes of Co deposit depends greatly on the pH of electrolyte. We reported that pH electrolyte play a key role in nucleation and early growth of Co deposits and Co grow *via* intermediary state. In this light, to perform electrochemically deposits with desirable properties, it's necessary to control the pH of electrodeposition process. Voltammetry characteristics are also discussed with attention given to the hydrogen evolution reaction (HER) process.

EXPERIMENTAL

Electrochemical experiments were carried out in a conventional three-electrodes cell. The reference electrode was a saturated calomel electrode mounted in a Lugging capillary. All potentials are referred to this electrode. The counter electrode was platinum wire. A rectangular plate of platinum was used as working electrode. The exposited surface of this later electrode is about 0.4 cm^2. Prior to each experiment, the working electrode was cleaned ultrasonically and sequentially in acetone, methanol and distilled water for 15 min and finally activated in hydrochloric acid for 2 min. All solutions were freshly prepared with water which was distilled twice. Cobalt

was deposited from chloride bath containing boric acid, its composition was shown in Table-1. The electrodeposition of cobalt was performed at overpotential deposition (OPD) using a Volta Lab 40 potentiostat/galvanostat controlled by a PC. The bath was stirred by nitrogen gas flow before electrodeposition of cobalt. Electrochemical experiments were performed in quiescent conditions: Voltammetric experiments were carried out at 20 mV/s, scanning initially towards negative potentials. Only one cycle was run in each voltammetric experiment. Chronoamperometric experiments were performed from an initial potential at which no process occurred to a potential at which reduction occurred.

TABLE-1
MOLAR COMPOSITION OF BATHS USED IN STUDY OF Co ELECTRODEPOSITION

Reagent	$CoCl_2$	NaCl	H_3BO_3	pH
Composition (mmol/L)	100	1000	500	Varied

X-ray diffraction phase analysis was performed on a INEL CPS120 diffractometer. The CuK_α radiation (λ = 1.5406 Å) was used, diffractogramms were obtained in the 2θ = 30-80º range. The temperature was fixed at 20 ºC during all experiments. Impedance measurements were performed with the same potentiostat/galvanostat used in voltammetric experiments. The amplitude of the alternated signal was 5 Mv in the frequency range of 10^5-10^{-3} Hz.

RESULTS AND DISCUSSION

Cyclic voltametry: In order to know the electrochemical behaviour and deposition potential of Co, the Pt electrode was scanned potentiodynamically in the solution containing 1 M NaCl, 0.5 M H_3BO_3 and 0.1 M $CoCl_2$ (solution with Co^{2+} ions). The voltammogramm was recorded at 20 mV/s, scanning from 0 V toward the negative direction and reversed at -1.4 V to positive direction and ended at 0.4 V. This first study was realized at 3.8 buffered pH. As can be seen in Fig. 1, the current becomes cathodic at about -1.0 V. During the forward scan toward the negative potentials, the cathodic current increases sharply once nucleation has begun. As the potential sweeps further to the cathodic side, the increase in corresponding cathodic current is related to the increase in the density nuclei and the crystal growth. At very negative potentials at about -1.3 V/SCE a significant increase in the cathodic current can be associated with the hydrogen evolution reaction (HER) process. Upon the sweep reversal in the anodic direction, the metal already deposited on the electrode surface continues to grow as a result of the reaction: $Co(II) + 2e^- \rightleftharpoons Co$. Reaction remaining thermodynamically and kinetically favourable, the current became anodic at about -0.5V *vs.* SCE. It then formed one great anodic peak, which corresponds to dissolution of deposited cobalt.

The voltammogramm presented the characteristic crossover between the current for the positive and negative sweeps, which suggests the presence of a nucleation and growth process[15]. The two crossovers between cathodic branches were clearly observable, the more cathodic crossover corresponds to nucleation potentials E_n, the second was the overcrossing potential E_c[16]. The inset of Fig. 1 shows the cyclic voltammogramm

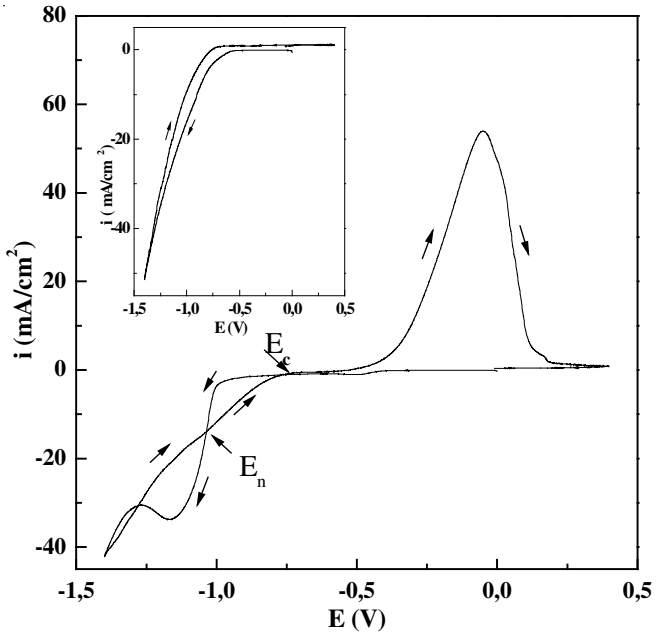

Fig. 1. Cyclic voltammogram for Pt surface in 1 M NaCl, 0.1 M $CoCl_2$, 0.5 M H_3BO_3 The inset shows voltammogramm in 1 M NaCl, 0.5 M H_3BO_3 (solution without Co^{2+} ions), pH ≈ 3.8, scan rate 20 mV/s

recorded for the solution containing only 0.5 M H_3BO_3 and 1 M NaCl (solution without Co^{2+} ions), the same conditions of scan rate and potential range were applied. As it can be seen the only cathodic current associated to the hydrogen evolution reaction appears early (at about -0.5 V). This behaviour may be due to the inhibition process caused by adsorbed complexes of cobalt on the surface electrode.

Chronoamperometric measurements and mechanism of nucleation process: Chronoamperometric measurements were realized in three solution with different values of pH (2.0, 3.1 and 4.0), by stepping up the potential from open circuit to a potential of -1.0 V. At this potential the reduction of cobalt ions closely proceeds. A family of current transients obtained at these values is shown in Fig. 2a.

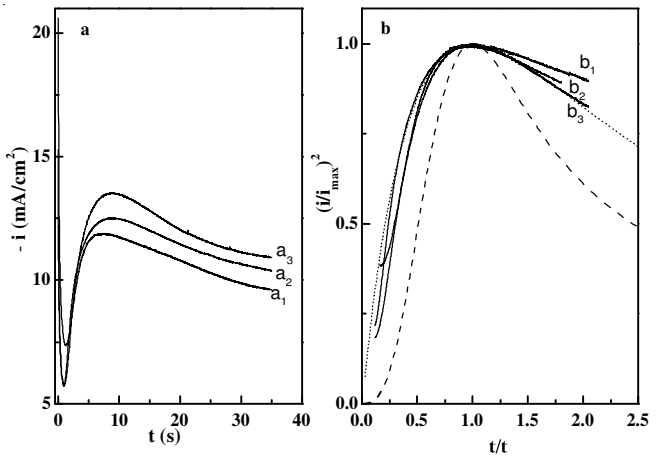

Fig. 2. (a) Current transients for cobalt electrodeposited from solution shown in Table-1. a_1: pH = 2 a_2: pH = 3.1 a_3: pH = 4. (b) Comparison between the theoretical non-dimensional plots for instantaneous (dotted line) and progressive nucleation (dashed line) and experimental current transients (b_1) pH = 2 (b_2) pH = 3.1 and (b_3) pH = 4

The shape of the recorded curves is a typical response of an electrochemical nucleation and growth process. At short deposition times, there is a falling current transient corresponding to the charging of the double layer followed by a rising current due either to growth of a new phase and/or to an increase of the number of nuclei. As the nuclei grow, the overlap of neighboring diffusion zones gives rise to a current maximum (t_{max}, i_{max}) which is followed by a decaying portion as predicted by the Cottrell equation[17-20]. Regarding the pH effect, the important difference is slower diffusion current decay (Fig. 2a_1) and the maximum of the current was reached at short time. Slower decay of diffusion current was the result of the significant contribution of hydrogen reduction current to the overall current and the short time at which the current reached it maximum was the result of shielding effect of hydrogen evolved on the surface of cobalt reducing the nuclei area available for continuation of cobalt deposition[21,22]. It is clear that H_{ads} was present at applied potential and local pH varied continuously.

In general, for the electrochemical growth process, the growth mechanism of the deposition of metals onto foreign substrates takes place at 3D island growth (Volmer-Weber). Models for electrochemical deposition onto a foreign substrate usually assume that nucleation occurs at certain specific sites on the surface and the nucleation mechanism is generally described in terms of either instantaneous or progressive nucleation[23]. The theoretical model proposed by Scharifker and Hills[24] is applied to distinguish between the instantaneous and progressive nucleation processes. Experimental chronoamperometric data is used by representing in a non-dimensional plot $(i/i_{max})^2$ *versus* t/t_{max}. The results are compared with the theoretical plots resulting from the following equations:

$$\frac{I^2}{I_{max}^2} = \frac{1{,}9542}{t/t_{max}}\left\{1-\exp\left[-1{,}2564\left(t/t_{max}\right)\right]\right\}^2 \qquad (1)$$

For instantaneous nucleation followed by three Dimensional diffusion-limited growth and

$$\frac{I^2}{I_m^2} = \frac{1{,}2254}{t/t_m}\left\{1-\exp\left[-2{,}3367\left(t/t_m\right)^2\right]\right\}^2 \qquad (2)$$

For progressive nucleation followed by three dimensional diffusion-limited growth[24,25]. The maximum current, i_{max}, corresponds to the time, t_{max}, at which the maximum current is observed. Also, t, in eqns. (1) and (2) is the time with respect to the onset of the deposition current. That's, t is corrected for the induction time, t_0. Fig. 2b compares the experimental results obtained at -1.0 V *versus* SCE, with the two limiting cases of the theoretical three-dimensional nucleation growth models. It can be seen in this illustration that nucleation process of Co on Pt surfaces was classified as instantaneous just for pH = 4 (curve b_3). For pH = 3.1 (curve b_2) the nucleation followed the instantaneous mechanism only when t exceeded t_{max} this means the contribution of hydrogen evolution reaction was not negligible at the beginning of the process. At pH = 2 (curve b_1), the situation was in disagreement with the theoretical model described by Scharifker and Hills.

Structural properties: Fig. 3 a, b and c shows the X-ray diffraction patterns of the cobalt films deposited at solution pH 2, 3.1 and 4.0 respectively. The bath temperature is fixed at 20 ºC and the applied potential is -1.0 V. At all selected pH range, several peaks were detected, indicating the polycrystalline structures. As can be seen at pH = 2 the electrodeposited film consisted of mixture of Co_{hcp} and Co_{fcc} crystallographic phases, however their peaks were very small (Fig. 3a). If electrodeposition was conducted at pH = 3.1 and 4, the Co_{cfc} variety was a tendency to disappear. The related Co_{hcp} was considerably more pronounced, (Fig. 3 c,d), the corresponding peak was higher and Co deposit was with better oriented crystals. The width of the peaks is small, indicating a good crystallization state with a large grain sizes.

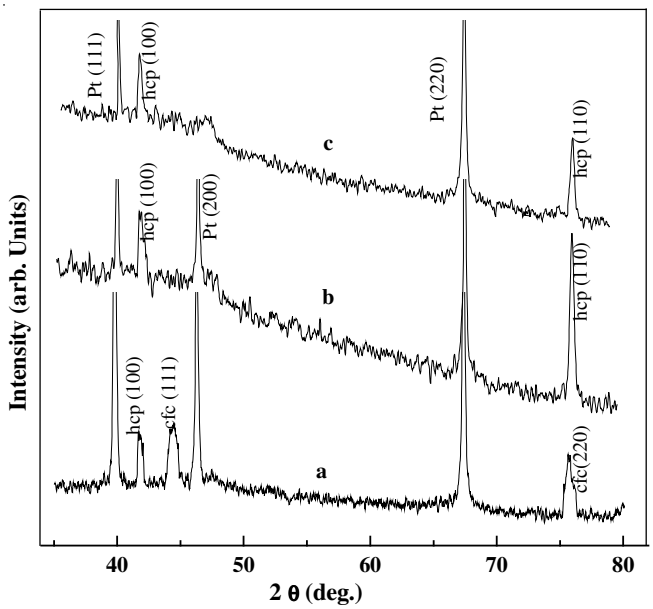

Fig. 3. X-ray diffraction (XRD) patterns of electrodeposited Co from solution shown in Table-1. (a) pH = 2.0, (b) pH = 3.1, (c) pH = 4.0

Assuming a homogeneous strain across crystallites, the size of microcrystallites can be estimated from the full width half maximum (FWHM) values of diffraction peaks. An average crystallite size could be obtained using the Scherrer formula[26,27] for crystallite size broadening of diffraction peaks:

$$\frac{0.94\lambda}{\beta\cos\theta}$$

where λ is the X-ray wavelength, θ the Bragg angle and β the FWHM of the diffraction peak. The results are reported in Table-2.

TABLE-2
XRD ANALYSIS OF ELECTRODEPOSITED COBALT AS FUNCTION OF ELECTROLYTE pH AT 20 ºC

pH	hcp(100)	hcp(110)	cfc(111)	cfc(220)
2.0	195.58	–	114.83	108.21
3.1	170.05	183.27	–	–
4.0	189.43	198.12	–	–

Electrochemical impedance measurements: Fig. 4 a, b, c displayed the EIS results obtained at previous pH values, at -1.0 V deduced from steady-state polarization curves realized

for the three pH values (not shown here). It could be seen that the difference in EIS curves is obvious. The impedance plot for the pH solution of 2.0 (Fig. 4a) shows a capacitive loop (100 Hz) and an inductive feature (below 1 Hz). This later is ascribed to the presence of adsorbed species and generally was referred to H_{ads} or Cl^-_{ads} on the electrode surface and consequently the cobalt reduction occurs *via* the initial formation an adsorbed Co(I) intermediate $Co(OH)_{ads}$ or $CoCl_{ads}$. At 3.1 pH value (curve b) the feature was changed and indicates the presence of a second capacitive loop at low frequency (1 Hz) The low frequency arc might be associated to the conversion of adsorbed species (H_{ads} to H_2 or $CoCl_{ads}$ to Co). This conversion would be very fast and no inductance feature is seen at low frequencies.

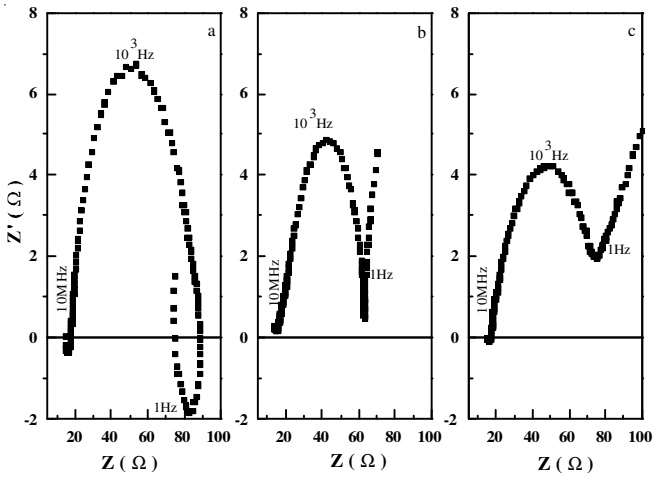

Fig. 4. Electrochemical impedance spectra of Pt surface in 0.1 M $CoCl_2$, 0.5 M H_3BO_3 at -1 V: (a) pH = 2, (b) pH = 3.1, and (c) pH = 4.0

In the last solution with pH = 4.0, the second loop disappeared and changed by straight line indicate the "Warburg" behaviour which is characterized by an important thick of the diffusion layer as described in literature[28,29].

Conclusion

The electrodeposited of cobalt from chloride bath to investigate the effect of pH as important relevant factor in electrodeposition. We have shown that the crystallographic structure depends closely to the pH of electrolyte. At low pH (≈2) the Co_{fcc} phase is privileged even the electrodeposited film contains the mixture of Co_{fcc} and Co_{hcp} phases. It have been concluded that an increasing in pH 3 < pH < 4, the Co_{fcc} fraction don't hold on and disappears and replaced by Co_{hcp} structure. The Co_{hcp} was considerably more pronounced, for pH > 2 the corresponding Co deposit was with better oriented crystals and growing of crystallites occurs with large grain size. the HER is not negligible for pH = 2 its influence is clear in nucleation study. It was found that nucleation mechanism is in good agreement with instantaneous theoretical model when pH exceeds the 2 value. Cyclic voltammetry and electrochemical impedance spectroscopy results suggest that a number of intermediate adsorbed complexes and adsorbed hydrogen are involved. The impedance spectra are characterized by the presence of a semicircle feature at high frequencies and by inductance feature at low frequencies and at low pH (≈2). This inductance feature is due to the formation of H_{ads} or Cl_{ads}. At high pH the inductance feature gives way to a capacitance feature at low frequencies indicating the fast step of desorbed species and at last the diffusion control of the process.

ACKNOWLEDGEMENTS

This work is supported by the Université Ferhat Abbas de Sétif, Algeria and the Université de Rennes1, France.

REFERENCES

1. J.H. Kefalas, *Plating*, **54**, 543 (1967).
2. T. Homma, Y. Kurokawa, M. Yammoto and T. Osaka, *J. Surf. Finish. Soc. Jpn.*, **44**, 1099 (1993).
3. A. Sahari, A. Azizi, N. Fenineche, G. Schmerber and A. Dinia, *Surf. Rev. Lett.*, **3**, 391 (2005).
4. J. Rivas, A.K.M. Bantu, G. Zaragoza, M.C. Blanco and M.A.L. Quintela, *J. Magn. Mater.*, **249**, 220 (2002).
5. D.H. Qin, M. Lu and H.L. Li, *Chem. Phys. Lett.*, **350**, 51 (2001).
6. M. Cerisier, K. Attenborough, E. Gedryka, M. Wojcik, S. Nadolski, C. Van Haesendonk and J.P. Celis, *J. Appl. Phys.*, **89**, 7083 (2001).
7. R.M. Bozorth, *Phys. Rev.*, **26**, 390 (1925).
8. P. Watts, *Trans. Am. Electrochem. Soc.*, **29**, 395 (1916).
9. E. Gomez and E. Valles, *J. Appl. Electrochem.*, **29**, 805 (1999).
10. J.L. Bubendorff, C. Meny, E. Beaurepaire, P. Panisod and J.P. Bucher, *Eur. Phys. J. B*, **17**, 635 (2000).
11. M. Cerisier, K. Attenborough, J.P. Celis and C. Van Haesendonk, *Appl. Surf. Sci.*, **166**, 154 (2000).
12. C.Q. Gui and J.Y. Lee, *Electrochim. Acta*, **40**, 1653 (1995).
13. J.S. Sallo, *J. Electrochem. Soc.*, **109**, 1040 (1962).
14. J.S. Judge, *Plating*, **53**, 441 (1966).
15. A. Sahari, A. Azizi, N. Fenineche, G. Schmerber and A. Dinia, *Mater. Chem. Phys.*, **108**, 345 (2007).
16. S. Fletcher, C.S. Halliday, D. Gates, M. Westcott, T. Lwing and G. Nelson, *J. Electroanal. Chem.*, **159**, 267 (1983).
17. A.N. Correia, S.A.S. Machado and L.A. Avaca, *J. Electroanal. Chem.*, **488**, 110 (2000).
18. J. Chunxin, G. Oskam and P.C. Searson, *Surf. Sci.*, **492**, 115 (2001).
19. L. Heerman and A. Tarallo, *J. Electroanal. Chem.*, **470**, 70 (1999).
20. A. Sahari, A. Azizi, G. Schmerber, M. Abes, J.P. Bucher and A. Dinia, *Catal. Today*, **113**, 257 (2006).
21. L.T. Romankiw and T.A. Palumbo, in eds.: L.T. Romankiw and D.R. Turner, Electrodeposition Technology, Theory and Practice, ECS, NJ, p. 13 (1988).
22. E.B. Budevski, in eds.: B.E. Conway, J.O.M. Bockris, E. Yeager, S.U.M. Kahn and R.E. White, Comprehensive Treatise of Electrochemistry, Plenum Press, New York, Vol. 7, p. 399 (1983).
23. G. Oskam, J.G. Long, A. Natarajan and P.C. Searson, *J. Phys. D*, **31**, 1927 (1998).
24. B.R. Scharifker and G.J. Hills, *Electrochim. Acta*, **28**, 879 (1983).
25. E. Bosco and S.K. Rangarajan, *J. Electroanal. Chem.*, **134**, 213 (1982).
26. C. Hammond, The Basics of Crystallography and Diffraction, Oxford University Press, Oxford (1997).
27. R.D. Tilley and D.A. Jefferson, *J. Mater. Chem.*, **12**, 1 (2002).
28. A.J. Bard and L.R. Faulkner, Electrochimie Principes, Méthodes et Applications, Paris, New York p. 354 (1983).
29. B. Tremillon, Electrochimie Analytique et Réactions en Solution, Masson Paris Tome 2, p. 183 (1993).